CrossMark

The numerical method for solving the transport equations in HgCdTe heterostructures using the non-equilibrium distribution functions

**Krzysztof Jóźwikowski[1] · Alina Jóźwikowska[2] ·
Michał Nietopiel[1]**

Abstract This paper presents a numerical method for solving the set of transport equations in semiconductor heterostructures by using the non-equilibrium distribution function for electrons and holes. This method enables the calculation of carrier concentration, carrier mobility and entropy by integrations in the space of wave vectors. In the same way the electrical current density and density of entropy currents are determined. The influence of quasi-Fermi energy gradients for electrons and holes and the gradient of temperature on the physical parameters of the heterostructure is taken into account.

1 Introduction

Usually semiconductor devices work in non-equilibrium conditions caused by electrical biasing and optical excitations. The flows of electric carriers and energy are driven by gradients of intense state parameters; quasi-Fermi energies for electrons and holes $\nabla\Phi_n(\vec{r})$ and $\nabla\Phi_p(\vec{r})$ respectively, and the gradient of temperature ∇T. These gradients can have a significant impact on the non-equilibrium distribution functions determining the statistical

---

✉ Krzysztof Jóźwikowski
    krzysztof.jozwikowski@wat.edu.pl

1   Institute of Technical Physics, Military University of Technology, ul. Kaliskiego 2,
    00-908 Warsaw, Poland

2   Faculty of Applied Informatics and Mathematics, Warsaw University of Life Science SGGW, ul.
    Nowoursynowska, Warsaw, Poland

🙂 Springer

probability that the electrical carrier has position $\vec{r}$ and wave vector $\vec{k}$. However, in commercially available simulators the non-equilibrium distribution functions do not contain these gradients, while one can find other non-equilibrium approaches including standard hydrodynamic transport and hydrodynamic transport with six moments of the Boltzmann transport equation (for example Grasser et al. 2001). Typically, the non-equilibrium distribution functions for electrons and holes with these gradients are derived by solving the kinetic Boltzmann equation, as it was done for example in the classical work (Marshak and van Vliet 1984). We have shown (Jóźwikowski et al. 2015), that functions derived in such way are only an approximation of more general terms. To derive them we had postulated a modified variational principle for the semiconductor heterostructure in steady state conditions being the composition of the Massieu function with the Gyarmati's principle. This proposed principle for conduction band electrons in steady state conditions reads as:

$$\int_V \lambda_e dV = \int_V \left\{ s_e - \frac{u_e}{T} + \frac{\Phi_n}{T} n + \bar{\tau}_e [\sigma_{s_e} - \Psi_e] \right\} dV = \max \tag{1}$$

here s_e is the density of electron entropy, n is electron concentration, u_e is the density of electron energy, T the temperature, Φ_n is the quasi Fermi energy for electrons, $\bar{\tau}_e$ is the mean electron relaxation time, σ_{s_e} is the efficiency of the source of electron entropy, V is the volume of the device and Ψ_e is the dissipation function in force representation (see Gyarmati 1967, 1969; Verhas 2014; Onsager 1931a, b; Onsager and Machlup 1953). Functional Eq. (1) achieves maximum value if the function λ_e satisfies the Euler–Lagrange equation, which means:

$$\frac{\partial \lambda_e}{\partial f_e} = 0 \tag{2}$$

The solution of Eq. (2) is the following non-equilibrium distribution function for electrons:

$$f_e\left(\vec{r}, \vec{k}\right) = \cfrac{1}{1 + exp\left(\cfrac{-\chi(\vec{r}) - e\Psi(\vec{r}) + \varepsilon_e^k\left(\vec{k}\right) - \Phi_n(\vec{r}) - \bar{\tau}_e(\vec{r})\frac{\hbar}{m_e^*(\vec{r})}\vec{k}\cdot\nabla\Phi_n(\vec{r}) + \frac{1}{6\left(m_e^*\right)^2 k_B}\bar{\tau}_e^2(\vec{r})\hbar^2 k^2\frac{(\nabla\Phi_n)^2}{T}}{k_B\left[T(\vec{r}) + \bar{\tau}_e(\vec{r})\frac{\hbar}{m_e^*(\vec{r})}\vec{k}\cdot\nabla T(\vec{r}) - \frac{1}{6(m_e^*)^2 k_B}\bar{\tau}_e^2(\vec{r})\hbar^2 k^2\left(\frac{\nabla\Phi_n\cdot\nabla T}{T} + \frac{s_e(\vec{r})(\nabla T)^2}{n(\vec{r})}\frac{}{T}\right)\right]}\right)} \tag{3}$$

A similar formula holds for non-equilibrium distribution function for holes, derived by this same method as for electrons:

$$f_h\left(\vec{r}, \vec{k}\right) = \cfrac{1}{1 + exp\left(\cfrac{\chi(\vec{r}) + e\Psi(\vec{r}) + \varepsilon_h^k\left(\vec{k}\right) + E_g(\vec{r}) + \Phi_p(\vec{r}) - \bar{\tau}_h(\vec{r})\frac{\hbar}{m_h^*(\vec{r})}\vec{k}\cdot\nabla\Phi_p(\vec{r}) + \frac{1}{6\left(m_h^*\right)^2 k_B}\bar{\tau}_h^2(\vec{r})\hbar^2 k^2\frac{(\nabla\Phi_p)^2}{T}}{k_B\left[T(\vec{r}) + \bar{\tau}_h(\vec{r})\frac{\hbar}{m_h^*(\vec{r})}\vec{k}\cdot\nabla T(\vec{r}) - \frac{1}{6(m_h^*)^2 k_B}\bar{\tau}_h^2(\vec{r})\hbar^2 k^2\left(\frac{\nabla\Phi_p\cdot\nabla T}{T} + \frac{s_h(\vec{r})(\nabla T)^2}{p(\vec{r})}\frac{}{T}\right)\right]}\right)} \tag{4}$$

In this paper distribution functions for ionized donors N_D^+ and acceptors N_A^- are expressed in a standardized form [see for example (Blakemore 1962)]. In relations (3) $\chi(\vec{r})$ denotes electron affinity, m_e^* it's effective mass, e elementary charge, Ψ electrical potential,

T temperature, s_e density of electron entropy, $\hbar$ Planck's constant, k_B Boltzmann's constant, n electron concentration, Φ_n quasi- Fermi energy for electrons, E_g is energy gap, $\bar{\tau}_e$ denotes mean relaxation time, $\vec{r}$ is the position vector and $\vec{k}$ is the wave vector. Subscripts p and h in Eq. (4) relate to the holes. Electron kinetic energy $\varepsilon_e^k\left(\vec{k}\right)$ and heavy hole kinetic energy $\varepsilon_h^k\left(\vec{k}\right)$ are expressed by Kane's relations (Kane 1957). Due to the scalar products $\vec{k} \cdot \nabla\Phi_n$, $\vec{k} \cdot \nabla\Phi_p$ and $\vec{k} \cdot \nabla T$ the functions expressed by Eqs. (3) and (4) are not even in $\vec{k}$. However in the analyzed structures ∇T is very small, so also expressions containing it can be omitted. Therefore integrating their product with the $\vec{k}$ in the first Brillouine's zone (BZ) allows to determine the density of carrier current and the density of entropy current. In the case of HgCdTe two different scattering mechanisms, for electrons and holes, i.e. scattering on ionized impurities as well as scattering on polarized optical phonons (Nag 1980; Lundstrom 1990) mainly limit the relaxation time. We have presented the detailed description of relaxation time for electrons and holes in HgCdTe in our previous paper (Jóźwikowski et al. 2004). If we consider the small values of gradients of $\nabla\Phi_n$, $\nabla\Phi_p$ and ∇T and expand relations (3) and (4) into Taylor series one obtains these same expressions as those obtained by (Marshak and van Vliet 1984). The physical parameters of HgCdTe can be found at (Capper and Garland 2011).

2 Method of numerical analysis

Our goal is to determine the physical parameters of devices, through the appointment of non-equilibrium distribution function. To reach it one has to solve the following non-linear system of transport equations, namely Poisson equation, continuity equation for electrons and holes, and the equation of energy balance, with suitable boundary conditions on the detector's surface and its electric contacts (see for example Parrot 1996; Jóźwikowski et al. 2010). In this paper we have considered Ohmic contacts and Neumann's boundary conditions on the surface beyond contacts. We have assumed constant temperature on the detector's surface and electric contacts, the same as in the environment.

$$\nabla^2\Psi = -\frac{e}{\varepsilon\varepsilon_0}\left(N_D^+ - N_A^- + p - n\right) - \frac{1}{\varepsilon}\nabla\Psi\nabla\varepsilon \tag{5}$$

$$\frac{\partial n}{\partial t} = \frac{1}{e}\nabla\vec{j}_e + G - R \tag{6}$$

$$\frac{\partial p}{\partial t} = -\frac{1}{e}\nabla\vec{j}_h + G - R \tag{7}$$

$$c_V\frac{\partial T}{\partial t} = -\nabla\left(Tj_{s_e}\right) - \nabla(Tj_{s_h}) + \nabla\chi\nabla T - \nabla(\Phi_n j_e) + \nabla(\Phi_p j_h) + G^{opt}E_g + G^{opt}\tilde{\varepsilon}_{e,opt}^k$$
$$+ G^{opt}\tilde{\varepsilon}_{h,opt}^k \tag{8}$$

The numerical solution of the set (5, 6, 7, 8) is obtained by using the Newton iterative methods. For this purpose we use our own computer programmes where the cell-centred finite volume method (FVM) as a discretization method is applied. G^{opt} denotes the optical generation rate, $\tilde{\varepsilon}_{e,opt}^k$ and $\tilde{\varepsilon}_{h,opt}^k$ is the average kinetic energy generated optically of electrons and holes, respectively, c_V is the specific heat, χ is the thermal conductivity

coefficient, G is the carrier generation rate, R is the carrier recombination rate, ε_0 is the permittivity of free space and ε is the dielectric constant. The G and R terms include interband Auger1 and Auger 7 mechanisms (Landsberg 1991). In addition, we have included the Shockley–Read–Hall processes caused by vacancies of metals and dislocations. A detailed description of the expressions for G and R being the function of quasi-Fermi energies and temperature can be found in our works (Jóźwikowski et al. 2010, 2012). G^{opt} is omitted in this paper.

Other quantities appearing in set (5, 6, 7, 8) are calculated by numerical integration in spherical space of wave vector k (Lundstrom 1990). For electrons, these values are expressed as follows:

$$n(\vec{r}) = \frac{1}{2\pi^2} \int\limits_0^{k_{max}} dk \int\limits_0^\pi k^2 \sin \Theta f_e\left(\vec{r}, \vec{k}\right) d\Theta \tag{9}$$

$$\mu_e(\vec{r}) = \frac{1}{n} \frac{e}{m_e^*} \frac{1}{2\pi^2} \int\limits_0^{k_{max}} dk \int\limits_0^\pi k^2 \sin \Theta \tau_e\left(\vec{r}, \vec{k}\right) f_e\left(\vec{r}, \vec{k}\right) d\Theta \tag{10}$$

$$\vec{j}_e(\vec{r}) = \frac{\hbar}{2\pi^2 m_e^*} \int\limits_0^{k_{max}} dk \int\limits_0^\pi k^2 \sin \Theta f_e\left(\vec{r}, \vec{k}\right) \vec{k} d\Theta \tag{11}$$

$$s_e(\vec{r}) = \frac{k_B}{2\pi^2} \int\limits_0^{k_{max}} dk \int\limits_0^\pi \sin \Theta \left\{ f_e\left(\vec{r}, \vec{k}\right) \ln f_e\left(\vec{r}, \vec{k}\right) + \left[1 - f_e\left(\vec{r}, \vec{k}\right)\right] \ln\left[1 - f_e\left(\vec{r}, \vec{k}\right)\right] \right\} k^2 d\Theta \tag{12}$$

$$\vec{j}_{s_e}(\vec{r}) = \frac{k_B}{2\pi^2} \int\limits_0^{k_{max}} \frac{\hbar \vec{k}}{m_e^*} dk \int\limits_0^\pi \sin \Theta \left\{ f_e\left(\vec{r}, \vec{k}\right) \ln f_e\left(\vec{r}, \vec{k}\right) + \left[1 - f_e\left(\vec{r}, \vec{k}\right)\right] \ln\left[1 - f_e\left(\vec{r}, \vec{k}\right)\right] \right\} k^2 d\Theta \tag{13}$$

Here $\vec{j}_e(\vec{r})$ denotes the density of electron current and $\vec{j}_{s_e}(\vec{r})$ is the density of electron entropy current. Similar expressions for quantities related with holes take forms:

$$p(\vec{r}) = \frac{1}{2\pi^2} \int\limits_0^{k_{max}} dk \int\limits_0^\pi k^2 \sin \Theta f_h\left(\vec{r}, \vec{k}\right) d\Theta \tag{14}$$

$$\mu_h(\vec{r}) = \frac{1}{p} \frac{e}{m_h^*} \frac{1}{2\pi^2} \int\limits_0^{k_{max}} dk \int\limits_0^\pi k^2 \sin \Theta \tau_e\left(\vec{r}, \vec{k}\right) f_h\left(\vec{r}, \vec{k}\right) d\Theta \tag{15}$$

$$\vec{j}_h(\vec{r}) = \frac{\hbar}{4\pi^3 m_h^*} \int\limits_0^{k_{max}} dk \int\limits_0^\pi k^2 \sin \Theta f_h\left(\vec{r}, \vec{k}\right) \vec{k} d\Theta \tag{16}$$

$$s_h(\vec{r}) = \frac{k_B}{2\pi^2} \int\limits_0^{k_{max}} dk \int\limits_0^{\pi} \sin\Theta \left\{ f_h\left(\vec{r},\vec{k}\right) \ln f_h\left(\vec{r},\vec{k}\right) + \left[1 - f_h\left(\vec{r},\vec{k}\right)\right] \ln\left[1 - f_h\left(\vec{r},\vec{k}\right)\right] \right\} k^2 d\Theta$$

(17)

$$\vec{j}_{s_h}(\vec{r}) = \frac{\hbar k_B}{2\pi^2 m_h^*} \int\limits_0^{k_{max}} dk \int\limits_0^{\pi} k^2 \sin\Theta \left\{ f_h\left(\vec{r},\vec{k}\right) \ln f_h\left(\vec{r},\vec{k}\right) + \left[1 - f_h\left(\vec{r},\vec{k}\right)\right] \ln\left[1 - f_h\left(\vec{r},\vec{k}\right)\right] \right\} \vec{k} d\Theta$$

(18)

We count the individual components of the current density in the standard way, for example x-th component of $\vec{j}_e$, reads as

$$j_{ex} = \frac{\hbar}{4\pi^3 m_e^*} \int\limits_0^{k_{max}} dk \int\limits_0^{2\pi} d\Phi \int\limits_0^{\pi} k^3 \sin^2\Theta f_e\left(\vec{r},\vec{k}\right) \cos\Phi d\Theta$$

(19)

The upper limit for the module of $\vec{k}$ vectors in our calculations for integrating in k space [in relations (9, 10, 11, 12, 13, 14, 15, 16, 17, 18, 19)] is the value of $k_{max} = 10^{10}$ m^{-1} and it is due to our practical experience.

While performing numerical simulations of semiconductor devices, we assume the knowledge of the spatial distributions of molar composition, electron affinity and doping. For those distributions we use the local electrical neutrality condition, which enables us to determine the initial value of the electric potential $\Psi_0(\vec{r})$. We then solve Poisson equation using iterative methods in order to determine the iterative corrections $\delta\Psi(\vec{r})$ for the electric potential in thermal equilibrium (Jóźwikowska 2008). This, in turn, allows the calculation of n, p, s_e and s_h by using relations (9), (14), (10) and (17), respectively. In conditions of thermal equilibrium distribution functions for electrons and holes are expressed by relations (3) and (4), respectively, but in this case $\Phi_n(\vec{r}) = \Phi_p(\vec{r}) = F$, where F is the Fermi energy and there is no gradients of intense state parameters. In biased heterostructures these gradients occur. Now, to determine the change of $\Psi(\vec{r}), \Phi_n(\vec{r}), \Phi_p(\vec{r}), T(\vec{r})$, with the change of the bias voltage, we have to solve the set of Eqs. (5, 6, 7, 8). These equations are solved now by fully coupled Newton iterations. It allows us to determine the iterative corrections $\delta\Psi(\vec{r}), \delta\Phi_n(\vec{r}), \delta\Phi_p(\vec{r})$ and $\delta T(\vec{r})$. Next, the corrected parameters $\Psi(\vec{r}) = \Psi(\vec{r}) + \delta\Psi(\vec{r}), \Phi_n(\vec{r}) = \Phi_n(\vec{r}) + \delta\Phi_n(\vec{r}), \Phi_p(\vec{r}) = \Phi_p(\vec{r}) + \delta\Phi_p(\vec{r}), T(\vec{r}) = T(\vec{r}) + \delta T(\vec{r})$ are inserted into Eqs. (9, 10, 11, 12, 13, 14, 15, 16, 17, 18) to calculate the corrected values of f_e, n, μ_e, $\vec{j}_e$, s_e, $\vec{j}_{s_e}$, f_h, p, μ_h, $\vec{j}_h$, s_h and $\vec{j}_{s_h}$.

3 Some numerical results

Below we present results of calculations of physical parameters of the cylindrical Hg$_{1-x}$Cd$_x$Te barrier MESA detectors with a radius of 30 µm (length of A'B line on Fig. 1), working at 300 and 230 K. Spatial distributions of mole fraction and donor and acceptor concentrations are shown along the axis of symmetry of the structure (line AA' in Fig. 1) in Fig. 2. All the spatial distributions of physical parameters of the structure are applied to distributions along AA' line. In the calculations we assumed that the dislocation density in
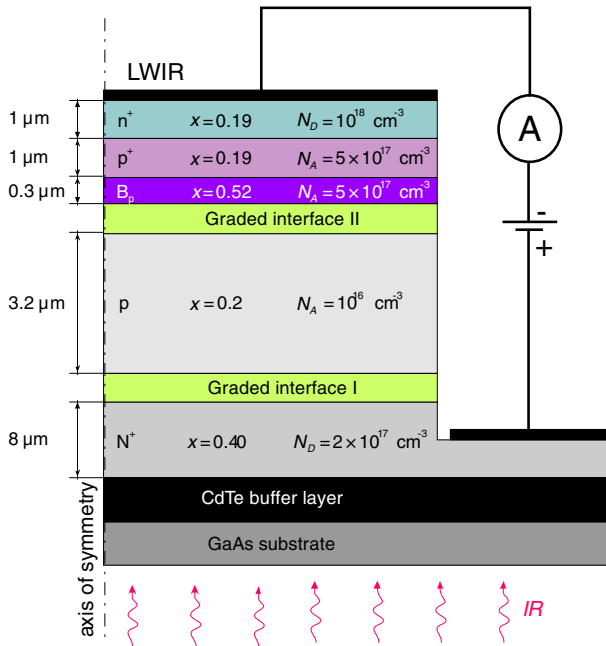
**Fig. 1** The architecture of the half cross-section of cylindrical barrier mesa structures
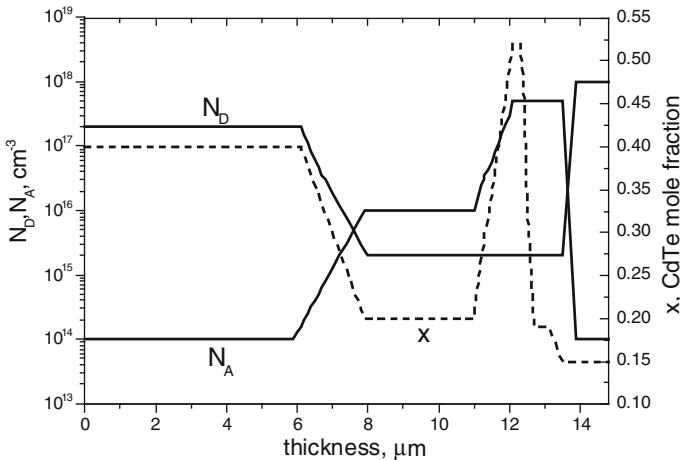
Fig. 2 Spatial distribution of mole fraction x donor concentration N_D and acceptor concentration N_A along AA' line axis of symmetry of the MESA structure

the whole structure is equal 10^6 cm^{-2} except for areas where there is a gradient of molar composition. In these regions the density of dislocations is increased according to the relationship proposed by (Yoshikawa 1988). The density of metal vacancies, being trap centres in $Hg_{1-x}Cd_xTe$, is assumed to be constant in all the heterostructures. We have considered their concentrations equal to 10^{14} cm^{-3} and 10^{15} cm^{-3}. Figure 3 shows calculated spatial distribution of carrier concentration and their mobility at 300 K in structure
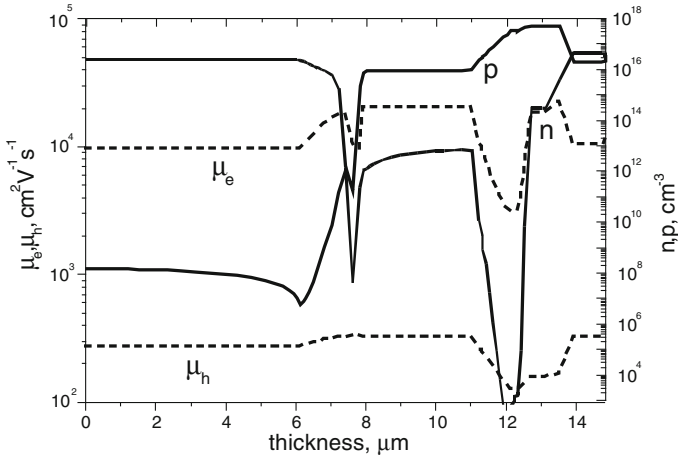
Fig. 3 Spatial distribution of calculated electron concentration n, hole concentration p, electron mobility μ_e and hole mobility μ_h after biasing with 1 V at 300 K

biased with 1 V in reverse direction. Spatial distribution of calculated energy band diagram and quasi Fermi energy for electron Φ_n and holes Φ_p, are shown in Fig. 4. Experimental and theoretical calculations of normalized current–voltage characteristics are compared in Fig. 5a, b. The calculations were performed taking into account the existence of serial resistance. Measured, normalized value of it at 300 K is equal 0.05 Ω cm^2. Figure 5a shows the results at 230 K. Good agreement between theoretical and experimental results is obtained for trap concentrations 10^{14}cm$^{-3} \leq N_T \leq 10^{15}$cm^{-3}. Figure 5a shows results at 300 K. However, detailed considerations need to take into account different trap concentration in different regions of the heterostructure. This is probably the reason of discrepancies between experimental and theoretical results for bias voltage in range 100–400 mV.
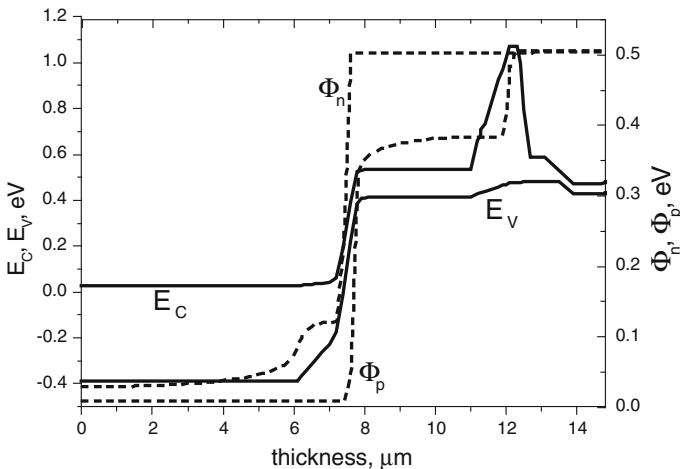
Fig. 4 Spatial distribution of calculated energy band diagram and quasi Fermi energy for electron Φ_n and holes Φ_p, after biasing with 1 V at 300 K
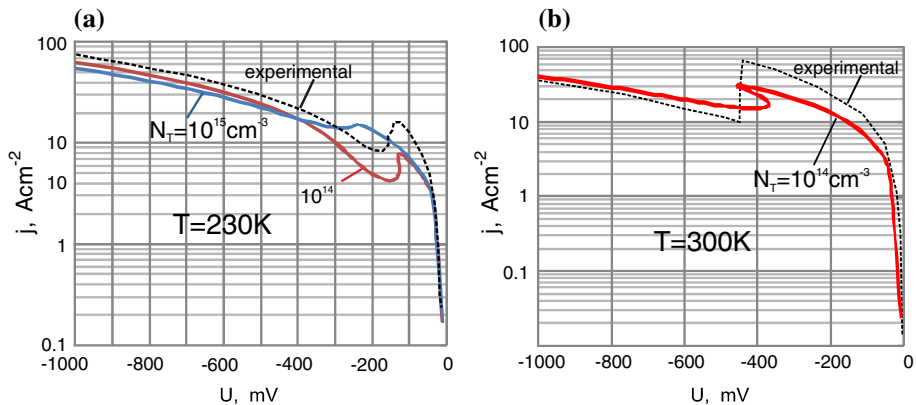
Fig. 5 Calculated (*solid lines*) and experimental (*dashed lines*) normalized current–voltage j(U) characteristics for presented barrier detector at 230 K (**a**) and 300 K (**b**). Calculations are carried assuming the normalized series resistance equal to 0.05 Ω cm^2 and trap density $N_T = 10^{14}$cm^{-3} and $N_T = 10^{15}$cm^{-3}

4 Conclusion

We have applied, derived earlier by ourselves, the non-equilibrium distribution functions for electrons and holes in the numerical modelling of barrier MESA infrared detectors. These functions are more general than those commonly obtained by solving the BKE and are valid also for strong gradients of quasi Fermi energies and the gradient of temperature. The proposed numerical method enables the calculation of physical parameters by the numerical integration of distribution function in the space of wave vector k. It is especially important to obtain proper values of the current densities. The method will be developed in future to distinguish the effective temperature of electrons, holes and lattice as well as the quasi-Fermi energies for electrons occupy donor, acceptor and trap centres.

References

Blakemore, J.S.: Semiconductor Statistics, pp. 117–175. Pergamon Press, Oxford (1962)

Capper, P., Garland, J. (eds.): Mercury Cadmium Telluride, Growth, Properties and Applications. Wiley, Singapore (2011)

Gyarmati, I.: On the relation between Onsager's and Prigogine's principles. Z. Phys. Chem. **234**, 371–378 (1967)

Grasser, T., Kosina, H., Gritsch, M., Selberherr, S.: Using six moments of Boltzmann's transport equation for device simulation. J. Appl. Phys. **90**(5), 2389–2396 (2001)

Gyarmati, I.: On the "governing principle of dissipative processes" and its extension to non-linear problems. Ann. d. Phys. **23**, 253–378 (1969)

Jóźwikowski, K., Musca, C.A., Faraone, L., Jóźwikowska, A.: A detailed theoretical and experimental noise study in n-on-p $Hg_{0.68}Cd_{0.32}Te$ photodiodes. Solid-State Electron. **48**(1), 13–21 (2004)

Jóźwikowska, A.: Numerical solution of the nonlinear Poisson equation for semiconductor devices by application of a diffusion-equation finite difference scheme. J. Appl. Phys. (2008). doi:10.1063/1.2982275

Jóźwikowski, K., Jóźwikowska, A., Kopytko, M., Rogalski, A., Jaroszewicz, L.: Simplified model of dislocations as a SRH recombination channel in the HgCdTe heterostructures. Infrared Phys. Technol. **55**, 98–107 (2012a)

Jóźwikowski, K., Kopytko, M., Rogalski, A., Jóźwikowska, A.: Enhanced numerical analysis of current-voltage characteristics of long wavelength infrared n-on-p HgCdTe photodiodes. J. Appl. Phys. (2010). doi:10.1063/1.3483926

Jóźwikowski, K., Kopytko, M., Rogalski, : The bulk generation-recombination processes and the carrier lifetime in mid-wave infrared and long-wave infrared liquid nitrogen cooled HgCdTe alloys. J. Appl. Phys. (2012b). doi:10.1063/1.4745872

Jóźwikowski, K., Jóźwikowska, A., Nietopiel, M.: The non-equilibrium distribution function for electrons and holes in semiconductor heterostructures in steady state conditions. Entropy **17**, 4110–4133 (2015)

Kane, E.O.: Band structure of indium antimonide. J. Phys. Chem. Solids **1**, 249–261 (1957)

Landsberg, P.T.: Recombination in Semiconductors. Cambridge University Press, Cambridge (1991)

Lundstrom, M.: Fundamentals of Carrier Transport. Volume X of Modular Series on Solid State Devices. Addison-Wesley, Boston (1990)

Marshak, A.H., van Vliet, K.M.: Electrical current and carrier density in degenerate material with non-uniform band structure. Proc. IEEE **72**, 148–162 (1984)

Nag, B.R.: Electron Transport in Compound Semiconductors. Springer, Berlin (1980)

Onsager, L.: Reciprocal relations on irreversible processes. I. Phys. Rev. **37**, 405–426 (1931a)

Onsager, L.: Reciprocal relations on irreversible processes. II. Phys. Rev. **38**, 2265–2279 (1931b)

Onsager, L., Machlup, S.: Fluctuations and irreversible processes. Review **91**, 1505–1512 (1953)

Parrot, J.E.: Thermodynamicstheory of transport processes in semiconductors. IEEE Trans. Electron Devices **43**(5), 809–826 (1996)

Verhas, J.: Gyarmati's variational principle of dissipative processes. Entropy **16**, 2364–2383 (2014)

Yoshikawa, M.: Dislocations in $Hg_{1-x}Cd_xTe/Cd_{1-z}Zn_zTe$ epilayers grown by liquid phase epitaxy. J. Appl. Phys. **63**, 1533–1540 (1988)